


## Article

# Optimal Cooperative Power Management Framework for Smart Buildings Using Bidirectional Electric Vehicle Modes

Rajaa Naji EL idrissi <sup>1</sup>, Mohammed Ouassaid <sup>1</sup>, Mohamed Maaroufi <sup>1</sup>, Zineb Cabrane <sup>2</sup>  
and Jonghoon Kim <sup>3,\*</sup>

<sup>1</sup> Engineering for Smart and Sustainable Systems Research Center, Mohammadia School of Engineers, Mohammed V University in Rabat, Rabat 10090, Morocco

<sup>2</sup> Laboratory of Innovative Technologies, National School of Applied Sciences of Tangier, Abdelmalek Essaadi University, Tetouan 93000, Morocco

<sup>3</sup> Department of Electrical Engineering, Chungnam National University, Daejeon 34134, Republic of Korea

\* Correspondence: whdgns0422@cnu.ac.kr; Tel.: +82-42-821-5657

**Abstract:** The high potential for implementing demand management approaches across multiple objectives has been significantly enhanced. This study proposes a cooperative energy management strategy based on the end-user sharing of energy. The proposed method promotes the intelligent charging and discharging of EVs to achieve vehicle-to-anything (V2X) and anything-to-vehicle (X2V) operating modes for both integrated and nonrenewable residential applications. These sharing modes have already been discussed, but resolution approaches are applicable to a specific use case. Other application cases may require additional metrics to plan the fleet of electric vehicles. To avoid that problem, this study proposes the MIP method using a robust Gurobi optimiser based on a generic framework for cooperative power management (CPM). Moreover, the CPM ensures an overall target state of charge (SoC) at leaving time for all the vehicles without generating a rebound peak in total grid power, even without introducing photovoltaic power. Two different methods are proposed based on the flow direction of the EV power. The first method only includes the one-way power flow, while the second increases the two-way power flow between vehicles, operating in vehicle-to-vehicle or vehicle-to-loads modes. A thorough analysis of the findings of the proposed model was conducted to demonstrate the robustness and efficiency of the charging and discharging schedule of several EVs, favouring a sharing economy concept, reducing peak power, and increasing user comfort.

**Keywords:** smart homes; demand-side management; electric vehicle; smart charging management; peak load; collective power management



**Citation:** Naji EL idrissi, R.; Ouassaid, M.; Maaroufi, M.; Cabrane, Z.; Jonghoon, K. Optimal Cooperative Power Management Framework for Smart Buildings Using Bidirectional Electric Vehicle Modes. *Energies* **2023**, *16*, 2315. <https://doi.org/10.3390/en16052315>

Academic Editor: Abu-Siada Ahmed

Received: 29 January 2023

Revised: 21 February 2023

Accepted: 23 February 2023

Published: 28 February 2023



**Copyright:** © 2023 by the authors. Licensee MDPI, Basel, Switzerland. This article is an open access article distributed under the terms and conditions of the Creative Commons Attribution (CC BY) license (<https://creativecommons.org/licenses/by/4.0/>).

## 1. Introduction

Intelligent demand-side management (DSM) system presents one of the most advanced and promising technologies for energy efficiency improvement in smart grids (SGs). It is primarily intended to reduce or shift electricity demand from peak periods based on dynamic pricing signals in order to achieve savings on the end-user side, mitigate grid overload, balance supply and demand, and ensure the reliability of the main grid [1]. This system also provides the flexibility of integrating renewable energy resources (RES) and electric vehicles (EVs) in the grid as future sustainable tools in both power supply and transportation sectors [2]. This increased use of EVs also enables local consumers to further reduce electricity bills by using them intelligently with the DSM. Although EVs have several environmental and social advantages, the adoption of large EVs charging in an uncontrolled way might have a negative impact on the network, e.g., they might affect the grid stability, raise the risk of overload burden, and reduce the advantage of a green electricity supply [3]. For that purpose, this research integrates DSM and the use of the home devices' schedule, as well as an optimization of EV charging/discharging to reduce the peak power and peak-to-average ratio (PAR).

In this regard, neighbourhood area networks (NANs) have been extensively considered in the literature [4,5]. They are composed of several smart homes containing a large set of controllable and noncontrollable appliances, energy storage units, and EVs. Home power management (HPM) strategies among entities of a NAN could have an important role to ensure common objectives, including the improvement of profits, the reduction of the energy dependency with the main grid, the increase of the resilience over faults, and the reduction of the peak-to-valley-load gap. Currently, there is an interest to adopt EVs to decrease power outages and the grid instability and to maximize the total energy efficiency [6]. Commonly, EV charging models are based on dynamic pricing signals, where the price relies on the demand, which encourages consumers to charge their EVs during low-demand periods to avoid electricity-cost peaks [2]. However, this can present an issue where an EV power is insufficient for an EV user's trips or it may create higher electricity peaks if a large number of users adopt the same electricity tariff requirements [7]. As a result, hereby, the formulation of an optimization problem to construct a community scaled DSM approach is proposed, considering multiple EVs' charging/discharging schedule, which promotes a sharing-economy concept, decreases peak power, and increases user comfort level.

### 1.1. Related Works

By and large, the impact of EV charging strategies on the power supply system has been widely discussed [7–9]. Basically, unscheduled grid-to-vehicle (G2V) charging strategies are devoted to being a short-term economical benefit. For that purpose, the development of unidirectional coordinated G2V charging techniques (Uni-G2V) and bidirectional EV power flow (Bi-V2X) alternatives are presented as key solutions to this problem [10,11].

The potential of EV charging strategies to alleviate the load demand during peak times has largely been investigated, especially peak load reduction, by making EV charging models based on dynamic pricing mechanisms [12]. In [12], the study used a ToU-price-based approach to motivate EV users to minimize their charging cycles during high-energy prices in order to reduce peak load. Hence, the consumers were price-takers who decided to activate their EV charging load in response to the TOU signal. Reference [13] demonstrated that the uncoordinated strategy based on charging price decrease may lead to major overloading of the power grid. Consequently, the neighbour constraints should be taken into consideration in the coordinated scheduling models. Peak load minimization based on dynamic pricing and the uncertainties of EV owners were presented in [14]. Dynamic cost signals were considered to decrease the peak load profile and increase the charging station's benefit. Results showed that the peak load based on a dynamic pricing model could induce an additional increase of more than 1500 euros. Furthermore, in [15] a hybrid scheduling approach was developed considering two targets, the minimization of daily charging prices and the peak-to-average ratio. Simulations demonstrated that the proposed model resulted in minimum financial effects by coupling the strengths of the two approaches more effectively. Moreover, the authors in [16] considered an optimization method for the EV's load demand regarding four aspects (frequency regulation profit, power quality, peak shaving, and charging cost). ToU tariffs were investigated to promote EV owners to supply auxiliary service and contribute to peak load shaving. Simulations proved the efficiency with respect to the grid performance development and benefit improvement. Differently, in [17], to minimize the peak load for power grids and eliminate the grid congestion at on-peak times, the charging scheduling of EVs was considered. The system aggregator had to give permission to the users for the charging scheduling of EVs.

Although the fitness functions are not similar in all these works, their common goal is to flatten the power demand profile to enhance the grid efficiency based on the coordinated EV charging frameworks. However, the modelling and development of power sharing among users given by a bidirectional vehicle-to-anything (V2X) framework has not been considered. In the proposed study, a CPM approach capable of optimizing the operation modes of EVs is proposed, including different home appliances' scheduling, energy sharing

among consumers, renewable generation input, in addition to Bi-V2X models when a large number of EVs are integrated.

In [18], a home energy management system was proposed to coordinate the schedules of different home energy resources during an outage period. The study considered the possibility of a bidirectional vehicle-to-home (V2H) mode for emergent supply backup during grid outages. Although results showed an improved performance of the home energy management (HEM) system to improve residential resilience, only a single home with a schedule issue was considered. The research presented in [19] revealed that a V2H framework can function optimally to satisfy both home and EV when properly handled, but only a single EV was considered. In [20], three different charging management strategies were conducted to increase solar power exploitation. The simulations showed that the proposed strategies improved the sharing of PV energy in charging energy by up to 62%, compared to 24% otherwise, resulting in a traditional G2V charge. However, that study did not consider a variable population of EVs and heterogeneous characteristics (such as state of charge (SoC) at the starting of the charging process, purposed SoC) were not provided. Reference [21] surveyed the new perspective on V2G development and future predictions. Another charging strategy was proposed in [22]. It aimed to alleviate power overloads of electric grid systems and minimize the cost using bidirectional energy sharing among vehicles (i.e., vehicle-to-vehicle). The obtained results proved that the proposed strategy obtained a greater performance than a benchmark algorithm. However, large-scale systems and renewable energy were not investigated in that work. In our previous study [23], a novel cooperative charging strategy for EVs based on a constraint programming algorithm was proposed. In addition to handling a heterogeneous and large-scale community in terms of EV peak charging load decrease and user satisfaction levels improvement, the examination of the model capability at both single and aggregated levels was considered. However, the exchange of energy between consumers did not occur. For this reason, this research extends the previous study and takes into consideration the limitations of existing works [18,20,22,23] by taking various EV charging/discharging modes into our problem scope as a novel contribution.

### 1.2. Main Contributions

Based on the above discussions, two novel cooperative power management strategies are proposed in this study to evaluate the impact of coordinated charging of EVs in a large user-oriented area. In addition to ensuring a reduction in peak load, it provides an expected overall SoC level at the departure time and improved cost savings. The main distinction between the two optimized CPM schemes relies on the EV power way direction. Firstly, an Uni-CPM scheme considers a unidirectional power direction. Secondly, a Bi-CPM scheme involves bidirectional power direction among vehicles, including V2V and V2L modes. The two CPM strategies are implemented and compared with the traditional EV charging strategy. The main contributions of this study can be summarized as follows:

- A hierarchical level of charging priority for EVs is established to coordinate the charging cycle of 1000 EVs based on their emergency status and the time required before users leave.
- An effective and coordinated decision-making strategy is established in order to promote energy sharing among different smart buildings according to different sharing rate preferences.
- A highly complex model that can adapt to large-scale buildings is proposed, including heterogeneous charging requirements, a set of controlled and uncontrollable electrical loads in addition to V2V and V2L applications.

### 1.3. Study Organization

The remainder of this study is organized as follows: Section 2 presents the mathematical formulation of the problem. Section 3 describes the modelling and solving strategies.

Then, the simulation results are illustrated in Section 4. Finally, the highlights and important findings are presented in Section 5.

### 2. Problem Formulation

The configuration of the proposed power system for an individual smart building is presented in Figure 1. In the figure, the smart layout of each household integrates a renewable energy system (solar power plant), a community power management (CPM) system, private essential domestic devices, bidirectional charging/discharging EVs, and a smart meter (SM) for two-way digital communication techniques. Moreover, for an effective scheduling, we categorized home appliances into three specific types according to the perspective of the HEM scheme:

- Non-controllable appliances: the HEM system is unable to control them, as they include the main needs of the users (television, refrigerator, etc.).
  - Interruptible appliances: the activation of their operation can be cut off and restarted later (pool pump, EV, etc.).
  - Non-interruptible appliances: their operation should be continued for a predefined period without a break until completing the job (washing machines, dishwasher, etc.).
  - Thermostatically controlled appliance (TCA): scheduled based on a predefined temperature interval. Thus, a TCA is fed by a determined range of energy (heating, ventilation and air conditioning (HVAC), electric water heater (EWH), etc.).
  - Energy storage loads: used to store and supply energy as required (battery, EV, etc.).
- An EV may be considered as an end-user appliance able to offer different advantages and challenges according to the nature of its charging operation. Multiple research studies have been conducted on EV charging models providing diverse perspectives. For example, a vehicle-to-home (V2H) mode provides a significant solution for load shaping at the end-user side, a vehicle-to-grid (V2G) mode leads to an efficient HEM process, and a vehicle-to-neighbour (V2N) mode offers excess EV energy to neighbours, among other EV operation modes. Hence, users can participate in their demand scheduling and profit from different options of energy usage.

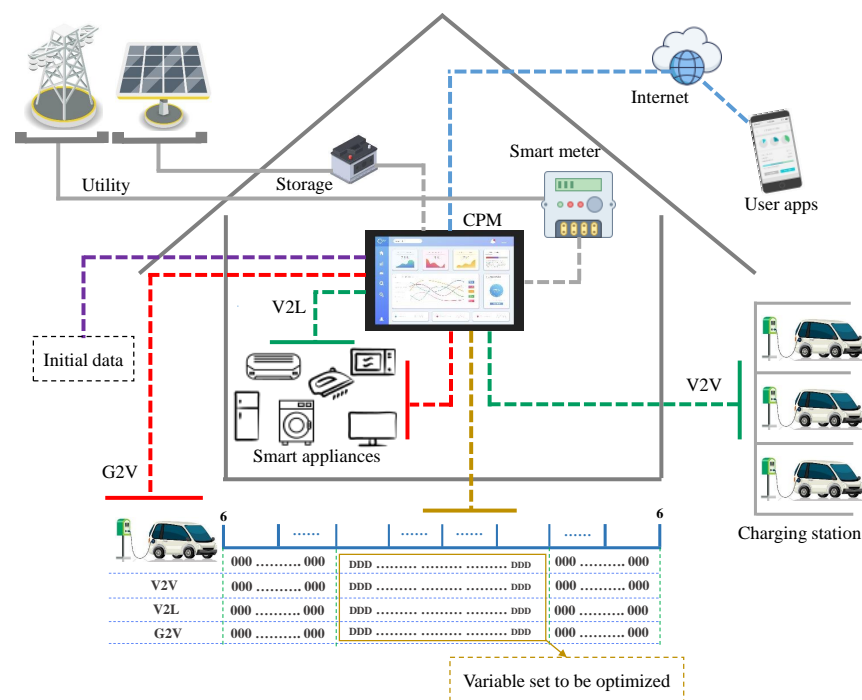


Figure 1. Overview of a single smart building.

In this section, the integration of each appliance with the proposed CPM strategy is explained.

### 2.1. Modelling of Thermostatically Controlled Appliance

As noted above, TCAs are classified as temperature-based control devices for consumer convenience. For HVAC systems, the energy consumption is measured by controlling the room temperature with a dead-band. Thus, the thermodynamic properties of the heat cycle are intrinsically related to the  $P_{HVAC}$  energy consumption, room temperature, solar irradiation, ambient air temperature, and other parameters. Based on the literature [24], Equations (1) and (2) describe the modelling deployed for HVAC monitoring.

$$T_{r,t} = T_{r,t-1} + \Delta t \cdot \frac{G_i}{\Delta c} + \Delta t \cdot \frac{C_{HVAC}}{\Delta c} \cdot S_{j,t}^{HVAC} \quad (1)$$

$$T_r^{\min} < T_r < T_r^{\max} \quad (2)$$

where:

$T_{r,t}$ , and  $T_{r,t-1}$  are the indoor room temperature at time  $t$  and  $t - 1$ , respectively;

$\Delta t$  is the time interval;

$G_i$  represents the heat gain rate of the house;

$C_{HVAC}$  is the HVAC thermal capacity;

$\Delta c$  is the energy needed to change the room air temperature;

$S_{j,t}^{HVAC}$  is the HVAC status at time slot  $t$ ; ( $S_{j,t}^{HVAC} = 1$  for the ON status, and  $S_{j,t}^{HVAC} = 0$  for the OFF status).

The operation of an HVAC system is limited by its nominal power consumption and the required temperature range set by consumers, i.e.,  $T_r^{\min}$  and  $T_r^{\max}$ . Note that Equation (1) estimates the indoor temperature in a consistent manner for 24 h time slots taking into account the thermal specifications of the air conditioning. Constraint 2 specifies the upper and lower acceptable internal temperature limits for the HVAC system, which are set considering the outdoor temperature conditions.

Similar to the HVAC model, the EWH model can also be defined as an input–output system where the the model output is the water temperature and the input signal is the operation status ( $S_{j,t}^{EWH} = 1$  for the ON decision, and  $S_{j,t}^{EWH} = 0$  for the OFF decision). Therefore, to ensure the comfort of the user, Constraint 3 sets the acceptable water heater range for the water temperature.

$$T_{outlet}^{\min} < T_{outlet,t} < T_{outlet}^{\max} \quad (3)$$

where  $T_{outlet}^{\max}$  and  $T_{outlet}^{\min}$  are the required maximum and minimum water temperature, respectively.

### 2.2. Modelling of Interruptible Appliances

#### Clothes Dryer

The modelling of a CD takes into consideration its operation time, i.e., the specified starting and ending times. This kind of controllable appliance can be time shifted to finalize their tasks in following period for incentive saving. The modelling of a CD unit is expressed as follows:

$$\begin{cases} \Delta H_{acc} < \Delta H_{req} \\ t > t_{CD}^{stat} \end{cases} \quad (4)$$

where  $\Delta H_{acc}$  denotes the accumulated drying cycle.  $S_{j,t}^{CD}$  is the responsive decision variable of the CD system. It equals one when switched off, otherwise it takes the value zero.

As demonstrated in Equation (4), a CD is generally operated about  $\Delta H_{req}$  and at a consumer-specified start time  $t_{CD}^{stat}$ . Appliance-level datasets are given in detail in [7,25,26].

### 2.3. Formulation of Objective Function

The on/off status related to EV charging decisions are given based on predefined individual and collective objectives. In this study, the power users were not considered to be electricity price followers, i.e., an EV consumption unit should make decisions considering the whole community constraints and individual priorities and not only in response to energy cost signals set by power grid operators. The objective function was given by Equation (5).

$$\min F(C) = \sum_{t=1}^T l_{basic,t} \lambda_{l,t} + \sum_{t=1}^T \sum_{i=1}^M (D_{i,t}^{EV,c} P_i^{EV} - D_{i,t}^{EV,V2V} P_i^{EV} - D_{i,t}^{EV,V2L} P_i^{EV}) \lambda_{l,t} \quad (5)$$

with

$$l_{basic,t} = \sum_{j=1}^N \sum_{t \in P_{ac}} l_{j,t}^{hvac} S_{j,t}^{HVAC} + \sum_{j=1}^N \sum_{t \in P_{WH}} l_{j,t}^{EWH} S_{j,t}^{EWH} + \sum_{j=1}^N \sum_{t \in P_{CD}} l_{j,t}^{CD} S_{j,t}^{CD} + \sum_{j=1}^N \sum_{t \in T} l_{j,t}^{fixed} \quad (6)$$

where:

- $D_{i,t}^{EV,c}$  denotes the charging status of  $i$ th EV at time  $t$ ;
- $D_{i,t}^{EV,V2L}$  and  $D_{i,t}^{EV,V2V}$  are the discharging decisions for V2L and V2V, respectively, for each single EV;
- $l_{j,t}^{hvac}$ ,  $l_{j,t}^{EWH}$ , and  $l_{j,t}^{CD}$  are the rated power demand of the  $j$ th HVAC device, EWH, and CD, respectively;
- $S_{j,t}^{HVAC}$ ,  $S_{j,t}^{EWH}$ , and  $S_{j,t}^{CD}$  are the decided status of the  $j$ th HVAC device,  $j$ th EWH, and  $j$ th CD at time  $t$ ;
- $l_{basic,t}$  presents the basic power demand at time  $t$ ;
- $\lambda_{l,t}$  is the power price at time  $t$ .

As expressed in Equation (6), the ultimate goal of this study was to minimize the operation cost of a power consumer  $j$  (i.e., a residential building), and maximize the profit of the overall operation system (i.e., EV aggregator or power grid).

## 3. Proposed Community Power Management Strategy

### 3.1. Traditional Immediate EV Charging Scheme

The traditional immediate EV charging scheme is a type of myopic strategy based on price information, that refers to uncoordinated decisions. In this charging mode, EVs are considered as a type of pure electric device for the electric power grid. Hence, an EV is charged directly once plugged into the main grid at its nominal charging power and stops charging when its battery pack is full or at its departure time from the charging grid. Indeed, for the whole electric grid, it presents a charging mode that aggravates the imbalances of supply–demand sides.

In particular, the EVs are recommended to be charged during the cheapest energy price periods through a scheduling process. The optimization problem is formulated by Equation (7), according to constraints (8)–(10).

Most users choose to charge their EV immediately after their day's work (5 p.m.). Hence, the charging demand generally occurs over the evening peak intervals, resulting in a higher demand on the total consumed electricity from the grid (rebound peaks).

The minimization problem is formulated as an independent and individual EV charging decision in Formula (7):

$$\min F(C) = \sum_{t=1}^T l_{basic,t} \lambda_{l,t} + \sum_{t=1}^T \sum_{i=1}^M (D_{i,t}^{EV,c} P_i^{EV}) \lambda_{l,t} \quad (7)$$

$$\lambda_{l,t} = \begin{cases} \lambda_{l,t}^{low}, & \text{if } t \in [t_{18}, t_{24}] \\ \lambda_{l,t}^{Avg}, & \text{if } t \in [t_1, t_8] \cup [t_{14}, t_{17}] \\ \lambda_{l,t}^{high}, & \text{if } t \in [t_9, t_{13}] \end{cases} \quad (8)$$

where  $\lambda_{l,t}^{low}$ ,  $\lambda_{l,t}^{Avg}$ ,  $\lambda_{l,t}^{high}$  are the off-peak, mid-peak, and on-peak prices, respectively.

$$D_{i,t}^{EV,c} = \begin{cases} 1, & \text{charging} \\ 0, & \text{idling} \end{cases} \quad (9)$$

Equation (8) ensures that the optimal EV charging status depends on the electricity cost intervals during the scheduling horizon, overlooking the effect of these decisions on the whole community profit and grid stability. Equation (9) represents the binary variable  $D_{i,t}^{EV,c}$  indicating the EV charging status.

$$SoC_{i,min} \leq SoC_{i,t} \leq SoC_{i,max}, t \in [t_i^{int}, t_i^{out}] \quad (10)$$

Constraint (10) expresses the permitted state of charge of the battery, where  $SoC_{i,max}$  and  $SoC_{i,min}$  express the maximum and minimum value of the state of charge, respectively;  $t_i^{int}$  is the start time of the  $i$ th EV, and  $t_i^{out}$  denotes the end time of the  $i$ th EV.

In this study, that charging scheme was considered as a benchmark, since it uses an uncoordinated EV charging strategy. Therefore, comparative studies between that scheme and two novel schemes, Uni-CPM and Bi-CPM, were conducted to highlight the obtained performance.

### 3.2. Unidirectional CPM Operation Mode (Uni-CPM)

By adopting the traditional charging scheme, the majority of consumers adhere to the same price signal. Hence, the loads usually operate outside of peak hours, which can result in a higher energy demand from the electricity grid. Therefore, the proposed Uni-CPM strategy was used to improve the performance of the system at a large scale (i.e., whole residential community) to meet the household electricity demand, coordinate EV charging, and mitigate the negative impacts of the uncoordinated EV charging strategy (e.g., rebound peaks, grid instability, etc.). In this study, the Uni-CPM model incorporated a power grid operator, EVs, CPM systems (CPMS), household devices, and other fundamental power system components.

In the Uni-CPM strategy, the allocation of the optimal charging start time of each  $EV_i$  was based on Equations (11) and (12), as a function of the required charging period ( $T_{i,req}$ ) and the sojourn period  $T_{i,stay}$ .

$$\beta_{i,urgency} = \frac{T_{i,stay}}{T_{i,req}} \quad (11)$$

$$Priority = \{EV_i, \dots, EV_M\} \quad (12)$$

Further,  $T_{i,req}$  and  $T_{i,stay}$  are defined by Equation (13) and Equation (14), respectively.

$$T_{i,req} = \left[ \frac{\eta_{battery} \cdot (SoC_i^{exp} - SoC_{i,t})}{P_{EV} \cdot \Delta t \cdot 100} \right] \quad (13)$$

where

$SoC_i^{exp}$  is the expected state of charge of the  $i$ th EV unit before the departure;

$SoC_{i,t}$  is state of charge level of the  $i$ th EV unit at the  $t$ th time period;

$\eta_{battery}$  is the efficiency of EV's battery;

$\Delta t$  is a time step;

$P_{EV}$  is the charging power of an EV (in kW).

$$T_{i,stay} = t_i^{out} - t_i^{int} \quad (14)$$

Note that  $\beta_{i,urgency}$  and *Priority* varied because of the daily start  $t_i^{int}$  and departure time  $t_i^{out}$  of each connected EV and  $SoC_{i,t_i^{int}}^{EV}$  (SoC value at the arrival time of the  $i$ th EV). When that index was the lowest, it meant that that EV did not have enough time to reach its expected  $SoC_i^{exp}$ , which explained its need to be plugged in first. Then, sorting the priority charging for each  $EV_i$  could be expressed by Equation (12).

$\beta_{i,urgency}$  was divided into two categories,  $\beta_{i,t}^{urgent}$  and  $\beta_{i,t}^{normal}$ , as follows:

- A set of emergency charging indexes for urgent EVs:

$$\beta_{i,urgency} = \left\{ \beta_{i,t}^{urgent}, \text{if } \beta_{i,urgency} < 1, T_{i,stay} < T_{i,req}, \forall t \right\} \quad (15)$$

- A set of emergency charging indexes for normal EVs:

$$\beta_{i,urgency} = \left\{ \beta_{i,t}^{normal}, \text{if } \beta_{i,urgency} \geq 1, T_{i,stay} \geq T_{i,req}, \forall t \right\} \quad (16)$$

The planning process based on Uni-CPM was carried out in five steps:

- **Step 1: Data input**

Primarily, it collects the EV charging load data for the following day, including:

$$\left\{ N, M, t_i^{int}, t_i^{out}, SoC_i^{exp}, SoC_{i,t_i^{int}}^{EV}, \Delta t, P_{EV}, \zeta_{bat,i}^c \right\}$$

- **Step 2: Initialization**

The initialization computes the sojourn period and the required period for a full charge for each EV's battery according to Equations (13) and (14).

- **Step 3: Charging Priority**

This step sorts the charging priority vector. After categorizing the EVs' load into two subgroups (Equations (15) and (16)), the charging priority array is ranked (Equation (12)), so that the charging priority can be accessed in ascending order. When the necessary time to get the required  $T_{i,req}$  is higher than  $T_{i,stay}$  ( $\beta_{i,urgency} < 1$ ), the goal is to prioritize the EV having a low  $\beta_{i,urgency}$ . Indeed, the objective of this step is to guarantee a total desired level at departure time for all the vehicles ( $SoC_{i,t_i^{out}}^{EV} = SoC_i^{exp}$ ).

- **Step 4: Charging time update**

It updates the new charging schedule order of EVs. Each  $EV_i$  is scheduled for charging at the target time slot.

- **Step 5: Optimization Stage**

(1.5) At this optimization stage, the decision variables of the proposed Uni-CPM scheme includes the operation status of each controllable appliance and the charging status of each  $EV_i$ . The objective function can be obtained by solving Equation (6). Here, the objective function is similar to the traditional charging strategy. However, extra subobjectives are considered as follows:

- An overall  $SoC_i^{exp}$  should be achieved at EV user departure time.
- Minimize the PAR expressed in (17) at both single and neighbourhood levels.
- Reduce the user dissatisfaction comfort level.
- Avoid the generation of rebound spikes after the proposed schedules.

(2.5) Thereafter, a judgement is rendered on whether the total maximum demand capacity exceeds the urgent EV charging demand or not. If yes, the system manager starts to plug in the EVs that need charging at the present time slot based on their priorities. If not, only EVs with higher charging preference levels can be charged.

(3.5) Upon completion of this step, the remaining EVs' satisfaction index  $\rho_i^{disat}$  is verified to judge if all EV loads are satisfied or not. If not, update the set  $t$  and go back



to step 2 again to select the following required time with updated EV data. Otherwise, the Uni-CPM program comes to the end.

To better clarify the above algorithm steps, the implemented Uni-CPM program is elaborated in Figure 2.

$$PAR = \frac{l_{peak}}{l_{average}} \quad (17)$$

where  $PAR$  is the ratio of maximum aggregate demand power  $l_{peak}$  to average aggregate consumed power  $l_{average}$ .

#### Bidirectional EV Operation Mode (Bi-CPM)

The second contribution of this study was to develop a smart collective model that could handle the various EV operation activities (charging/discharging). Hence, discharging statuses included V2L, and V2V, in addition to G2V charging statuses. The detailed mathematical formulation for the optimization problem is introduced in this section. Thus, the following assumptions were considered in the development of the proposed Bi-CPM model: (1) the studied vehicles were purely EVs; (2) the rated power of an EV corresponded to the EV charging or discharging power; (3) the reactive power of EVs was not included; (4) due to incentive goals, the electricity cost of the EV charging mode G2V and discharging modes (V2L and V2V) was similar.

#### A-Energy Constraints for EV Users' Side

The activity of recharging a single EV during its recharging duration should satisfy the EV user's desire for energy for movement.

Equation (18) indicates that an EV charge and discharge operation mode cannot be interrupted. So, at each time interval, an EV needs to be inactive, charging, or in one of its discharging activities (i.e., V2H, V2V, or V2L).

$$D_{i,t}^{EV,c} + D_{i,t}^{EV,V2L} + D_{i,t}^{EV,V2V} = \begin{cases} 0, \text{inactive} \\ 1, \text{either charging or discharging mode} \end{cases} \quad (18)$$

Additionally, the following constraint should be satisfied to guarantee that the discharging power of V2L and V2V will not flow into the power grid:

$$l_{basic,t} + \sum_{t=1}^T (D_{i,t}^{EV,c} P_i^{EV} - D_{i,t}^{EV,V2V} P_i^{EV} - D_{i,t}^{EV,V2L} P_i^{EV}) > 0 \quad (19)$$

Equations (20) and (21) represent the battery charge requirement for an EV, where  $SoC_i^{EV,\min}$  and  $SoC_i^{EV,\max}$  are usually set at 37.5% and 90% to extend the EV's battery life [18]. The time was set to  $T = [1, \dots, 24]$  with a resolution of one hour during a day, and  $N$  is usually equal to 1 for a single residential building.

$$SoC_i^{EV,\min} \leq SoC_{i,t}^{EV} \leq SoC_i^{EV,\max}, \forall t \in T, \forall i \in M \quad (20)$$

$$SoC_{i,t}^{EV} = SoC_{i,t_i^{\text{int}}}^{EV} + \frac{\zeta_{bat,i}^c P_i^{EV}}{C_i^{EV}} \sum_{t=t_i^{\text{int}}}^t D_{i,t}^{EV,c} - \frac{\zeta_{bat,i}^d P_i^{EV}}{C_i^{EV}} \sum_{t=t_i^{\text{int}}}^t (D_{i,t}^{EV,V2L} + D_{i,t}^{EV,V2V}) \quad (21)$$

where

$C_i^{EV}$  is the battery capacity of the  $i$ th EV;

$\zeta_{bat,i}^c$  and  $\zeta_{bat,i}^d$  are the charging and discharging efficiencies of the  $i$ th EV, respectively.

For the required energy from an EV user, Equation (22) states that the charging activity of an individual EV during its charging period should satisfy the expected energy of the EV user at departure time.

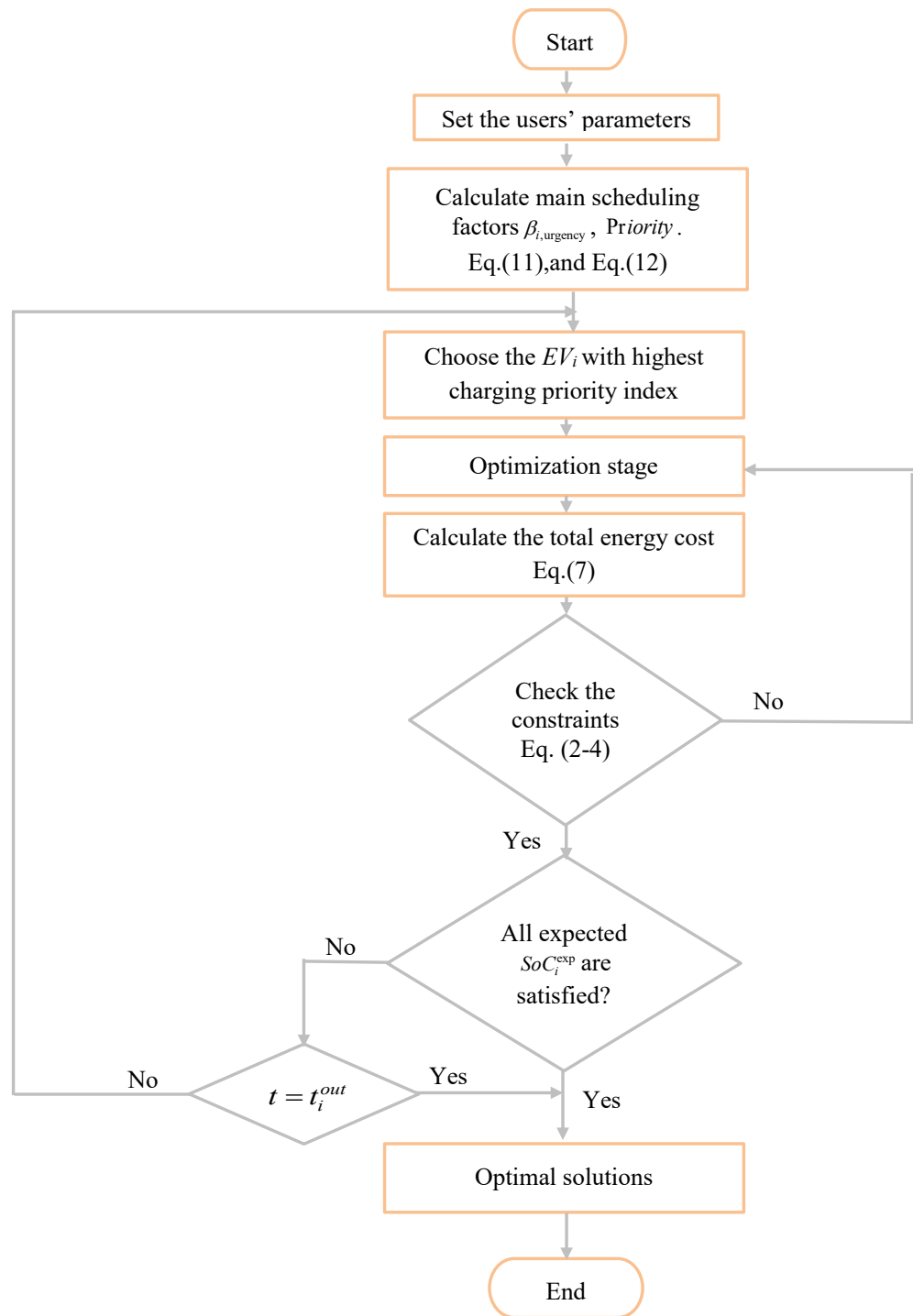


Figure 2. Flowchart of the proposed Uni-CPM scheme.

$$|SoC_{i,t_i^{out}}^{EV} - SoC_{i,ideal}^{EV}| \leq \epsilon, \epsilon \rightarrow 0^+ \tag{22}$$

where Equation (23) explains the calculation of the state of charge at  $t_i^{out}$  ( $SoC_{i,t_i^{out}}^{EV}$ ).

$$SoC_{i,t_i^{out}}^{EV} = SoC_{i,t_i^{int}}^{EV} + \frac{\zeta_{bat,i}^c P_i^{EV}}{C_i^{EV}} \sum_{t=t_i^{int}}^{t_i^{out}} D_{i,t}^{EV,c} - \frac{\zeta_{bat,i}^d P_i^{EV}}{C_i^{EV}} \sum_{t=t_i^{int}}^{t_i^{out}} (D_{i,t}^{EV,V2H} + D_{i,t}^{EV,V2L} + D_{i,t}^{EV,V2V}) \tag{23}$$

Equation (24) represents the V2V discharging mode at a time period  $t$ . Namely, the number of EVs acquiring energy from other vehicles during their plug-in time cannot

exceed the number of cars transferring energy to other EVs. This means that the total number of EVs operating in V2V mode each time should be equal to or greater than the total number of EVs operating in charge mode.

$$\sum_{i=1}^M D_{i,t}^{EV,c} - \sum_{i=1}^M D_{i,t}^{EV,V2V} \geq 0 \quad (24)$$

### B-Management of Charging/Discharging of EVs

For the above Bi-CPM model, both EVs charging and discharging statuses should be solved, in addition to controllable devices. Therefore, charging/discharging decisions were designed as Boolean variables attributed to the charging status  $D_{i,t}^{EV,c}$  or to the discharging  $D_{i,t}^{EV,V2L}$ , and  $D_{i,t}^{EV,V2V}$  for V2L and V2V, respectively, for each single EV.

Since different discharging scenarios and buildings were involved, a generic model was designed to conduct the optimization process for different operations of EVs, as displayed in Figure 3. The information, including electricity prices, available PV power, EVs' data, the preference of sharing activities (charging/discharging), and other main datasets were collected at the initial step of the proposed Bi-CPM program.

Based on the data acquired, the optimization problem was set. Next, it was resolved to get the charging/discharging solutions for the available EVs. It was assumed that the preferences of charging/discharging behaviours for various users could be adjusted according to practical requirements.

Moreover, calculating the emergency index, and sorting the charging priority array for the connected vehicle using Equations (11) and (12), the scheduling system used a self-consumption factor  $\alpha_i$  that was expressed as a function of available PV power and EV demand.

$$\alpha_i = \frac{P_{pv_i}}{P_{EV_i}} \quad (25)$$

As given in Equation (25),  $\alpha_i$  was expressed as an instantly available ratio between the available PV power and the total EV power demand. If the PV availability was sufficient to satisfy the EV charging power for the plugged vehicle  $\alpha_i \geq 1$ , the system took advantage of its internal production  $P_{pv_i}$ . Otherwise, if  $\alpha_i < 1$ , the extra PV power was supplied to other loads or injected into the following prioritized EV.

On the other hand, in the case where  $\alpha_i < 1$ , a V2V scheme was required. The EV with the lowest emergency index could be distributed to the plugged-in EV through the adoption of V2V scenarios.

During this discharging phase, EVs with higher  $SoC_{i,t}^{EV,int}$  and  $\beta_{i,urgency}$  levels (i.e.,  $\beta_{i,urgency} = \beta_{i,t}^{normal}$ ) shared a fraction of their energy with vehicles having a lower  $SoC_{i,t}^{EV,int}$  and  $\beta_{i,urgency} = \beta_{i,t}^{urgent}$ .

The difference compared to the Uni-PCM was that the bidirectional power stream was assigned by the Bi-CPM. This considered an EV's battery discharging toward a generic load (V2L or V2V), unlike the one-way power flow, which only took into account the direction of the energy source (the grid in our case or PV) to the EV.

### C-Solution Methodology

For the above Bi-CPM strategy, decision variables consisted of three parts: (1) the charging and discharging statuses; (2) the operation status of each controllable appliance; (3) the power consumed by the neighbours. These decision variables were encoded and expected to be solved for each single home in the studied community. Hence, each single home would have  $6 \times 24$  variables. Considering all these boolean decision vectors for the whole community of 1000 users required an enormous computational effort for the MIP model. MIP has been extensively applied to programming issues and is often the initial approach to address a new programming problem. However, to supplement the performance improvements of the MIP model, it is necessary to use them with modern solver technology.

To solve this problem, involving complex compromises between competing decisions and allowing a large number of possible solutions, only MIP has the power to find the best or optimal solution [27]. The Gurobi optimizer was employed to solve the proposed models in this study. The optimum solution of both Uni-CPM and Bi-CPM problems were found.

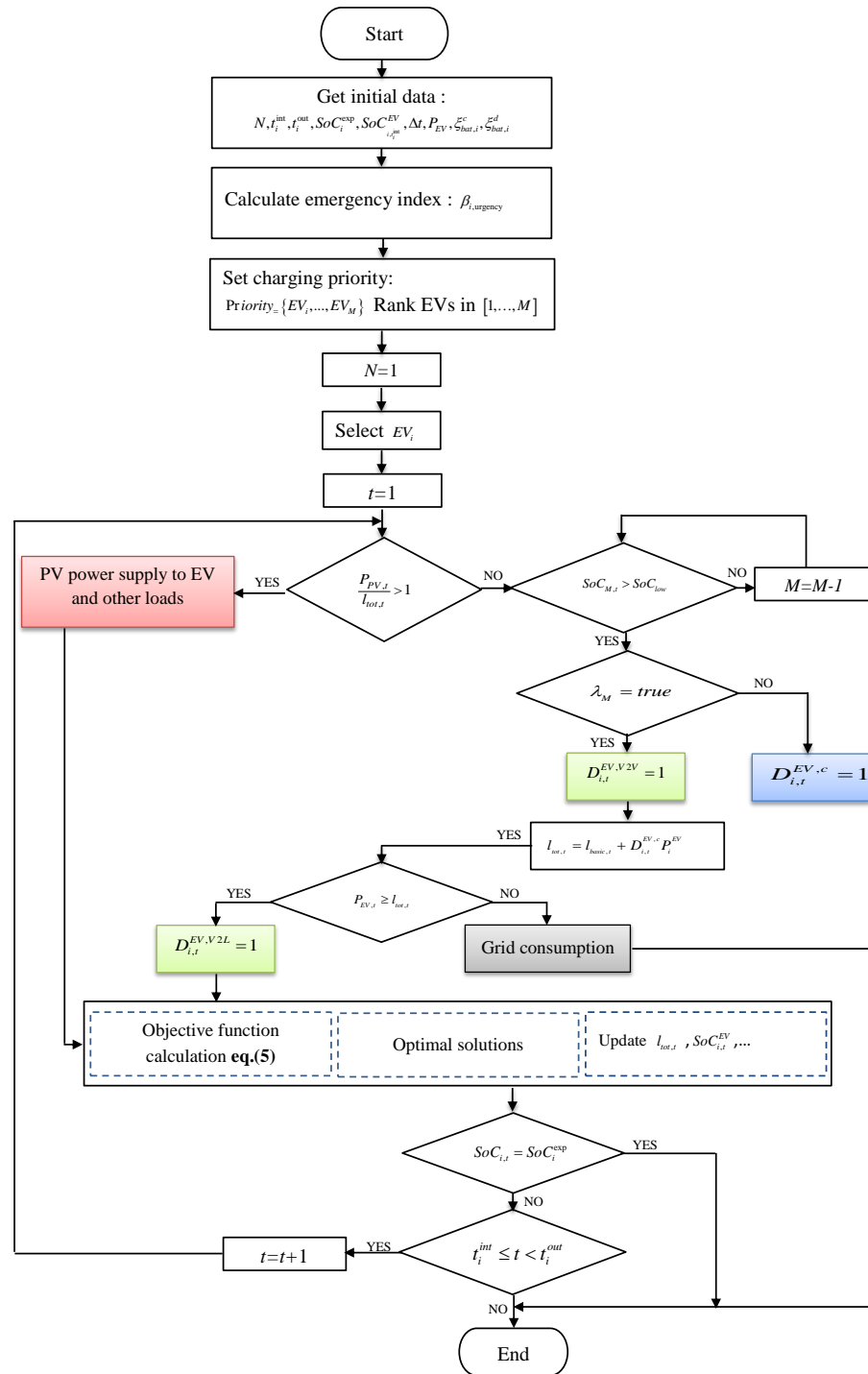


Figure 3. Flowchart of the proposed Bi-CPM scheme.

Algorithm 1 displays the key workflow steps for the MIP model using the Gurobi Optimizer.

**Algorithm 1** Workflow of MIP model for EV scheduling

---

```

1:  $m = \text{Model}(\text{"mip1"})$  # Create the MIP model
2: for  $i = 1 : M$  do
3:   for  $t = 1 : T$  do
4:      $D_{i,t}^{EV,c} = m.addVar(vtype = GRB.BINARY, name = D_{i,t}^{EV,c})$  # Create the variables
5:      $D_{i,t}^{EV,V2L} = m.addVar(vtype = GRB.BINARY, name = D_{i,t}^{EV,V2L})$ 
6:      $D_{i,t}^{EV,V2V} = m.addVar(vtype = GRB.BINARY, name = D_{i,t}^{EV,V2V})$ 
7:      $model.setObjective(F(C), GRB.MINIMIZE)$  # Set the objective
8:     Generate energy constraints for EV users' side # Add the model constraints
9:      $m.optimize()$  # Optimize the model
10:     $print(D_{i,t}^{EV,c}, D_{i,t}^{EV,V2L}, D_{i,t}^{EV,V2V})$  # Report result
11:   end for
12: end for

```

---

**4. Case Studies and Analyses**

In this part, the impact of the EV charging on the peak loads of power grid is discussed. The grid performance was evaluated in the presence of EVs with different operating modes: (1) the traditional immediate charging mode; (2) the proposed Uni-CPM operation; and (3) the novel developed Bi-CPM operation. Simulations were carried out using the python programming language.

A comparative analysis between the two novel strategies, Uni-CPM and Bi-CPM, and the benchmark immediate EV charging approach were performed to highlight the benefits of the proposed CPM. Since both Uni-CPM and Bi-CPM schemes aimed to alleviate the worst weaknesses occurring under the traditional immediate EV charging scheme, both approaches were simulated by taking into consideration heterogeneous conditions of EV users (departure time, expected state of charge, preference of participating in charging/discharging processes, etc.).

Moreover, different cases were analysed to assimilate the role of CPM integrated with the G2V and/or V2L and V2V modes as an alternative energy source on the efficient energy sharing and electricity tariffs reduction over the whole community of smart houses, respectively. The first case considered 1000 houses without PV production in which the G2V traditional charging model, coordinated charging model, and the V2L and V2V charging/discharging models were implemented. The second case corresponded to 1000 houses equipped with a PV energy source and also subject to the EV conventional charging, coordinated charging, and V2L and V2V charging/discharging. The different designed cases are shown in Table 1.

**Table 1.** Simulation cases and scenes.

Case 1: No Integrated PV			Case 2: Integrated PV	
Scenario 1	Scenario 2	Scenario 3	Scenario 4	Scenario 5
Traditional immediate charging scheme	Uni-CPM scheme	Bi-CPM scheme	Uni-CPM scheme	Bi-CPM scheme

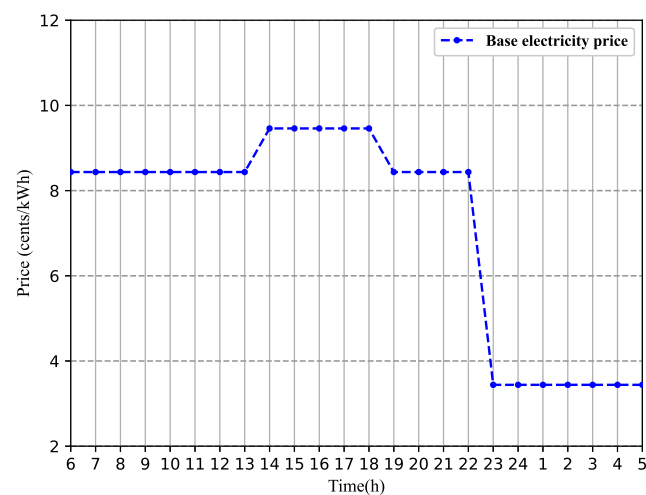
*Basic Parameter Settings*

To evaluate the performance of the proposed charging models, a complete day with a 24 h time horizon was considered, with a time granularity of 1 min. The EVs considered were private vehicles with a similar capacity of 24 kWh and nominal charging power of 3.3 kW. Both charging  $\zeta_{bat,i}^c$  and discharging  $\zeta_{bat,i}^d$  efficiency were set to 0.98. Table 2 depicts the main technical specifications of the simulated EVs. Based on existing works, the arrival of EV users was 6:30 p.m., while their departure times were taken randomly [23,25,28].

**Table 2.** Simulation parameters.

Parameter	Value	Parameter	Value
$t_i^{out}$ range	[20:00, 11:00]	$SoC_i^{EV,min}$	0.375
$t_i^{int}$ range	17:00	$SoC_i^{EV,max}$	1
$SoC_{i,i}^{int}$ range	[0.375, 0.65]	$\zeta_{bat,i}^c$	0.98
$\zeta_{bat,i}^d$	0.98	$P_i^{EV}$ (kW)	3.6
$SoC_i^{exp}$ range	[0.5, 0.1]		

In this study, the proposed models were used to optimize the charging and discharging statuses of EVs based on intervals of the initial  $SoC_{i,i}^{EV}$  and target state of charge  $SoC_i^{exp}$ , as given in Table 2. Figure 4 presents the electricity price signal used for the tests. As previously mentioned, this work aimed to develop a generic model that could perform in different smart buildings conditions. Therefore, the price vector was assumed for the testing objective, which meant that the prices could take other values and achieve the same performance. As can be seen in Figure 4, the high price period occurred during  $[t_9, t_{13}]$ . In addition, the studied NРАН involved 1000 consumers with a different rate of preference for the participating EVs ( $Pr_i$ ).

**Figure 4.** Price signal for simulation.

### A-Community of Buildings without PV:

In this case, the electricity demand in all houses was provided by the grid and EVs were also charged from the grid, i.e.,  $P_{PV}^{2L} = 0$ , and  $P_{PV}^{2V} = 0$ . The total grid power demand for the whole area based on the three EV scheduling strategies are given in Figure 5. According to the simulation outcomes (Figure 6c), the case of the “traditional immediate EV charging scheme” had the highest grid power demand compared to the two other strategies over the day. As most of EVs were directed to charge after 17:00 (i.e., when users return home after work), the uncoordinated behaviour of the parked EVs generated a high peak load in the total grid consumption. In addition, a higher grid power demand during 17:00–19:00 induced an increase in electricity fees imposed by selfish EV charging demand by charging each EV immediately after returning home without considering CPM as displayed in Table 3.

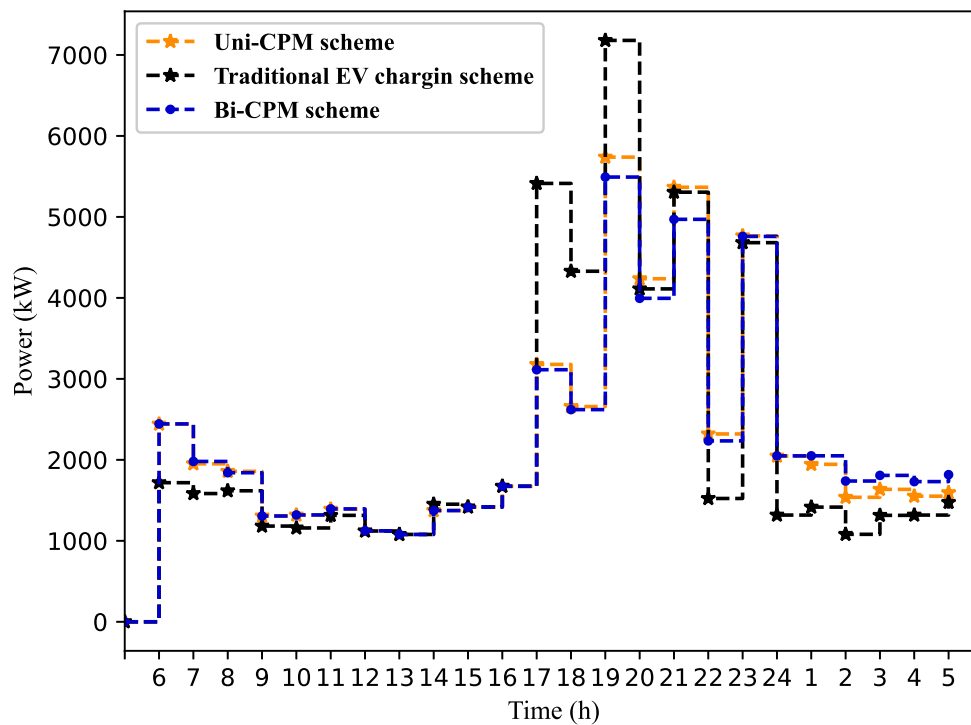
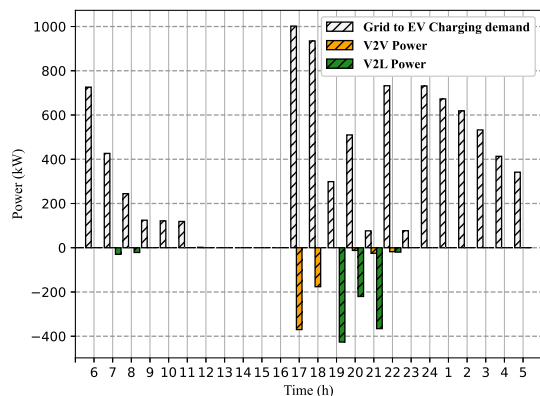
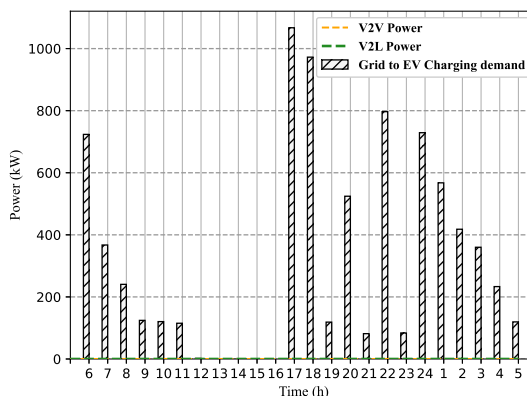


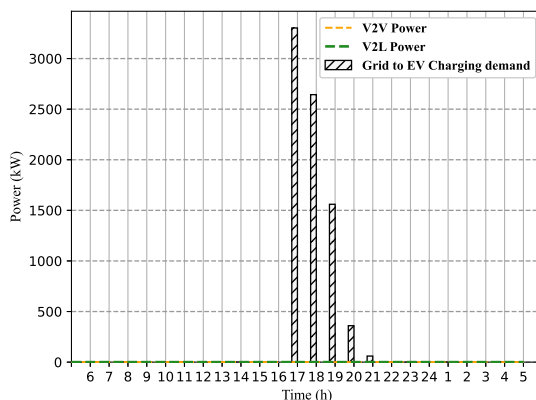
Figure 5. Total grid power consumption for the three schemes.



(a) Using the proposed Bi-CPM scheme.



(b) Using the proposed Uni-CPM scheme.



(c) Using uncoordinated EV charging scheme.

Figure 6. Obtained profiles in case1.

**Table 3.** Comparison of obtained performance under different schemes in case 1.

Scenario	PAR	Highest Peak Demand (kW)	Highest Peak Reduction (%)	Cost ( $\times 10^3$ Cents)	Cost Saving (%)
1	2.38	5491.29	23.51	385,285	6.9
2	2.48	5739	20	391,292	5.7
3	3.07	7179.41	-	413,692	-

In the proposed “Uni-CPM” (Figure 6b) and “Bi-CPM” (Figure 6a) schemes, the lowest EV total grid demands are shown over the day, because EVs were charged according to the CPM schemes, therefore it was profitable to charge EVs based on the whole community load demand and EV charging necessity. In the case where the charging and discharging ability of EVs were permitted, the EVs were directed to discharge when the load price was high, performed V2L (at 19:00–22:00), and chose to share in the V2V mode when price was also attractive (mid-peak period), without increasing the whole community peak load (depicted in Figure 5).

Furthermore, the PAR for the total buildings were 2.48 and 2.38 with Uni-CPM and Bi-CPM, respectively, implying a reduction of 6.9% in energy fees with EV sharing enabled. This shared EV power was used to decrease the total grid power demand by up to 23.51% as displayed in Table 3.

$$l_{basic,t} + \sum_{t=1}^T (D_{i,t}^{EV,c} P_i^{EV} - D_{i,t}^{EV,V2V} P_i^{EV} - D_{i,t}^{EV,V2L} P_i^{EV}) \leq l_{limit} \quad (26)$$

Although the huge capacity of the grid could supply a maximum demand capacity, the NRAN’s complex referred to a contract with a system manager to set a limited power consumption called the restricted demand capacity  $l_{limit}$ . Accordingly, this constraint imposed an upper limit to the total energy consumed in any time slot as expressed in Equation (26).

In another way, to better examine the efficiency of the proposed scheduling strategies, we evaluated the dissatisfying SoC level when the system coordinated all 1000 EVs under a lower restricted demand capacity (e.g., 4400–6500 kW). To measure the dissatisfaction level, a defined  $\rho_i^{disat}$  of the  $i$ th EV was expressed by Equation (27).

$$\rho_i^{disat} = SoC_i^{exp} - SoC_{i,t_i}^{int} \quad (27)$$

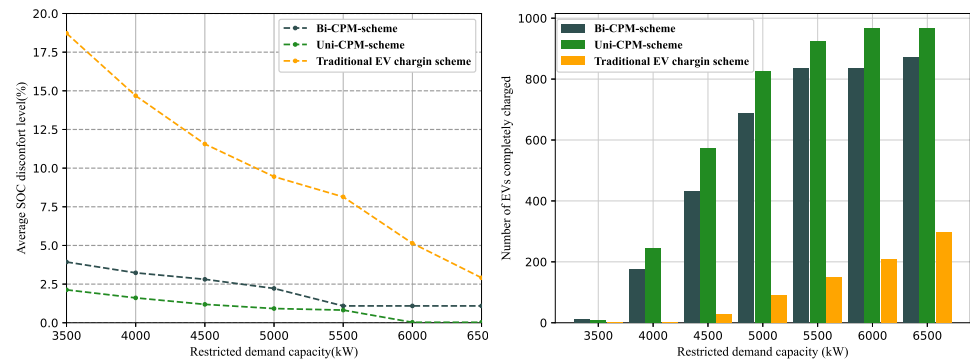
For a quantitative analysis of the dissatisfaction comfort index reduction, we evaluated two metrics,  $\rho_i^{disat}$  and the total number of EVs accommodated for a complete charge, which was measured by the average aggregate number of EVs achieving  $SoC_i^{exp}$ .

As shown in Figure 7b, the proposed Bi-CPM scheme indicated a significantly greater number of EVs hosted for a complete charge without exceeding the restricted power capacity, relative to the traditional EV charging scheme. With a limited power capacity of 5500 kW, the proposed coordination scheme could accommodate up to 837 EVs throughout the community.

It should be noted that the level of dissatisfaction  $\rho_i^{disat}$  and the number of indicted EVs had a compromise relationship between them in the proposed Bi-CPM scheme. In other words, a smaller  $\rho_i^{disat}$  could cause a larger number of EVs to completely charge in the proposed scheme. On the other hand, in the traditional EV charging scheme, using the contracted power capacity with all 1000 smart buildings, there was no EV completely charging under the smaller restricted power capacity (for example,  $l_{limit} = 3500$  kW).

Figure 7a exhibits the average level of  $\rho_i^{disat}$  for all 1000 EVs of the proposed CPM schemes as the limited power capability increased. It can be shown that the average dissatisfaction level decreased as the  $l_{limit}$  increased, and the proposed Uni-CPM system achieved a zero  $\rho_i^{disat}$  dissatisfaction level above  $l_{limit} = 6000$  kW.





(a) Average SoC dissatisfaction level. (b) Number of EVs completely charged.

**Figure 7.** Analysis of average SoC dissatisfaction level and number of EVs completely charged for all 1000 EVs.

As explained in Section 3, the challenge of energy sharing preference among users was quantified through the evaluation of EV charging/discharging cycles. The values of the  $Pr_i$  coefficient for the EV charging/discharging cycles were therefore simulated to examine the influence of the number of EVs participating in the economy sharing. Hence, the proposed Bi-CPM was analysed for different  $Pr_i$ 's and the simulation results including the total EV charging and discharging loads and the economic profit are presented in Figure 8.

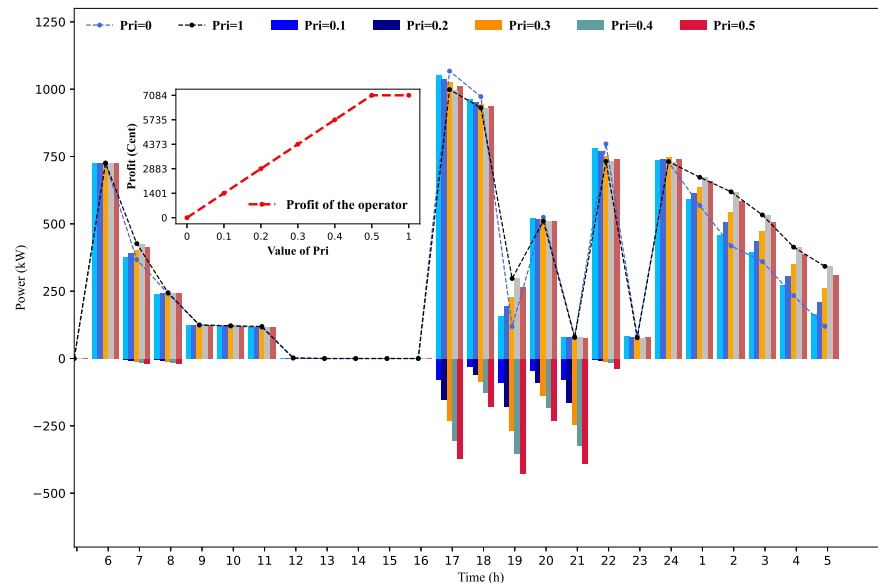


**Figure 8.** Simulation results of the EV charging/discharging loads with different  $Pr_i$ 's; the total cost profit improvement is shown in the small frame.

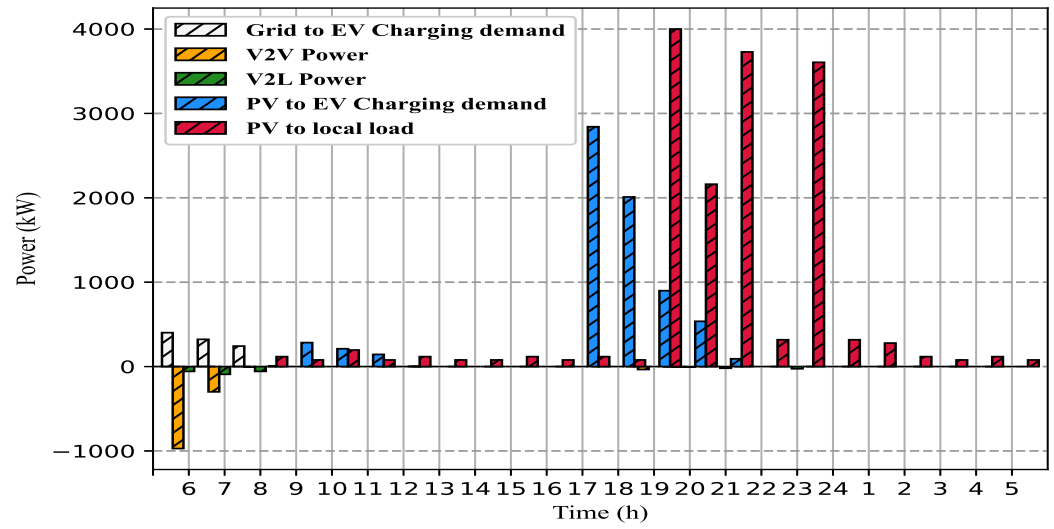
As can be seen from Figure 8, with a  $Pr_i$  increase, EVs preferred to perform more discharging cycles; therefore, the users intelligently selected to perform charging or discharging in adjacent time slots as  $Pr_i$  increased. In the case of  $Pr_i = 0$ , the details of the EV behaviours for that scenario were similar to those of the Uni-CPM model and the discharging cycles were excluded, since no EVs were selected to share. It can also be clarified from Figure 8 that the economic profit tended to raise more when  $Pr_i$  increased, while it presented smallest values when the value of EV sharing was less (i.e., with smaller  $Pr_i$ ).

The preference for sharing is thus a significant concern that can affect the EV charging/discharging actions and the operating costs of the power demand profile.

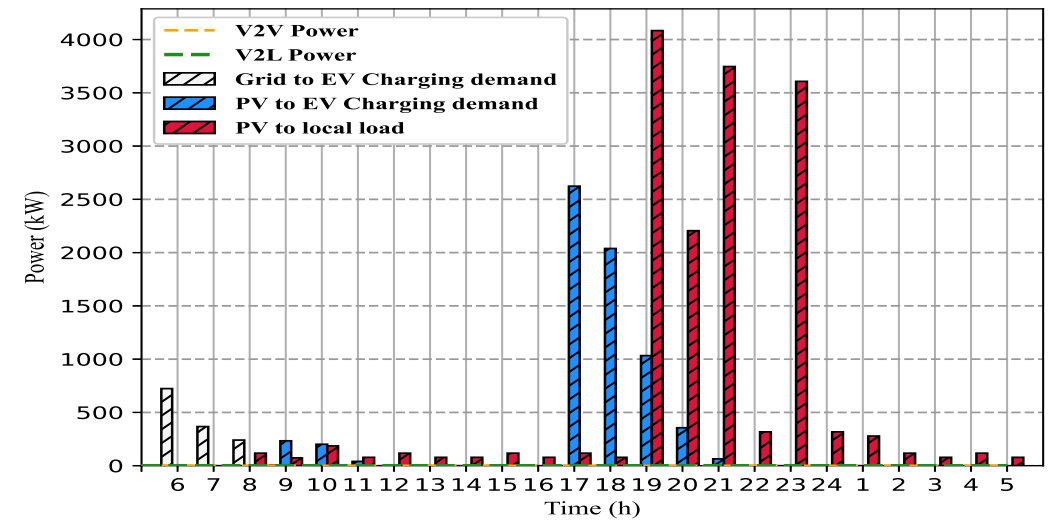
### B-Community of Buildings Equipped with PV

In this case, the daily electricity demand was preferably supplied by PV power. The grid offered power to charge EVs or others loads when the PV power was insufficient to meet the home load. The PV power supplied by the PV system installed at each home could also be delivered for both load demand usage and EV charging consumption.

Figure 9 illustrates the PV power demand consumed from household loads and PV-based charging of EVs. In Figure 9a, a great proportion of PV power was utilized to fulfil the resident load demand, demonstrating a minor difference among the two proposed CPM schemes.



(a) Using the proposed Bi-CPM scheme.



(b) The proposed Uni-CPM scheme.

Figure 9. Obtained profiles in case 2.

Using the proposed “Bi-CPM” scheme, more PV power was used to charge EVs during the time interval 17:00–21:00 than in the “Uni-CPM” scheme, since the charging demand of EVs was heavy due to the discharging operation of EVs. This indicated that the discharging power from EVs could be used for the charging demand of EVs. Accordingly, a great decrease of the total grid power consumption for EV charging was achieved through the proposed “Bi-CPM” scheme.

This was supported by the results from Table 4, by using PV power for the local demand and EV charging, the consumption cost was reduced by 3579 cents as the grid power demand was reduced. The supplied PV energy from EV batteries could shift from PV power production peak to power demand peak with peak shaving using the V2V and V2L modes of the Bi-CPM scheme. Thus, an effective improvement of the PV self consumption rate was a necessity. The PV consumption rate could be calculated using Equation (28), adopted from [29].

$$PV_{rate} = \frac{P_{PV}^{2L} + P_{PV}^{2V}}{P_{PV,t}^{Total}} \times 100 \quad (28)$$

where  $P_{PV}^{2L}$  represents the PV energy consumed by the loads,  $P_{PV}^{2V}$  is the PV energy used to charge the EV, and  $P_{PV,t}^{Total}$  is the total daily PV energy.

**Table 4.** Comparison of obtained performances under different schemes in case 2.

Scenario	PAR	Highest Peak Demand (kW)	Cost ( $\times 10^3$ Cents)	PV Consumption Rate (%)
4	1.8	2443	234,273	36.9
5	1.77	2441	230,694	36.5

Figure 10 shows the total electricity consumption provided by the grid, PV source, and EV sharing under the Bi-CPM and Uni-CPM schemes. It can be seen from Figure 10 that the V2L and V2V exchanges could cover a significant electricity demand requirement, thereby reducing the grid electricity consumption. It presented a positive signal for the development of the Bi-CPM scheme since the proportion of grid consumption in the Uni-CPM was larger than that of the Bi-CPM. Therefore, it can be depicted that the Bi-CPM scheme contributed to reducing the electricity cost, PAR minimization, and emission reduction.

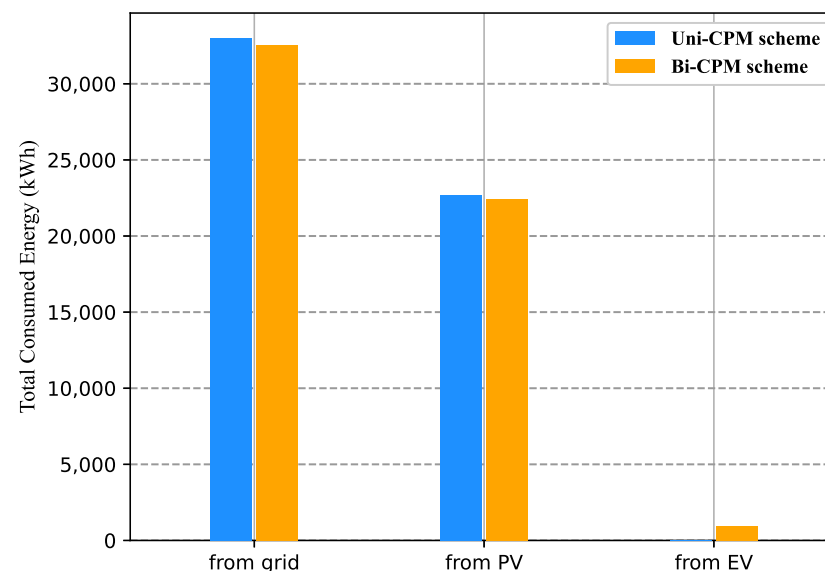


**Figure 10.** Total household electricity consumption provided in case 2 under Uni-CPM and Bi-CPM.

## 5. Conclusions

Cooperative power management among smart homes presents a major challenge in smart grid management. This study classified residential households into two main types and modelled each type based on their technical or thermal characteristics and the requirements of users, in order to satisfy users. Two novel EV charging management strategies operating in a CPM model were proposed. The two CPM strategies varied as a function of the power flow direction. The Uni-CPM only considered the grid to EV flow

direction. However, the Bi-CPM enabled a two-way power flow among loads and EVs (V2V and V2L), in addition to a smart EV charging scheduling to ensure an overall expected SoC at the leaving times of all users.

For this, a robust Gurobi optimizer based CPM was proposed to optimally manage the charging/discharging EVs' power flow to avoid peak demand, ensure electricity cost savings and minimal consumer dissatisfaction. Intensive simulations were carried out to evaluate the performance of the proposed strategies in which a traditional EV charging scheme was taken as a benchmark.

Results showed improvements of 967 EVs (Uni-CPM) and 837 EVs (Bi-CPM) in the number of EVs achieving an expected SoC at departure time, considering about 23.51% and 20% of highest peak reduction after implementing the Bi-CPM and Uni-CPM schemes, respectively.

Both emergency- and priority-based EV charging planning strategies resulted in savings of up to 5.7% and 6.9% over the traditional EV charging system. For the best-performing results, a PV integration was tested as a second case of the two proposed schemes in order to minimize external grid consumption. Considering the same conditions, the Uni-CPM and Bi-CPM schemes presented similar performances in terms of minimal peak load, PAR, and cost saving. By using the Bi-CPM scheme, the average consumption of the supplied network was lower than that of the Uni-CPM thanks to the bidirectional operation mode (V2V and V2L).

This research can be expanded into several directions. A first direction would be to manage several EV users within a common renewable energy, energy storage, and electricity grid, including the analysis of battery degradation levels over the life cycle of energy storage units and EV batteries. Second, a practical implementation of the proposed CPM framework for domestic applications should be validated by a test bench with a PV source and an EV connected to the electricity network, which is typical of modern intelligent buildings.

**Author Contributions:** Conceptualization, R.N.E.i. and M.O.; methodology, R.N.E.i., M.M. and M.O.; software R.N.E.i.; validation, R.N.E.i., M.O., J.K. and Z.C.; formal analysis, R.N.E.i., M.M. and Z.C.; investigation, J.K. and Z.C.; resources, M.O., Z.C. and J.K.; data curation, R.N.E.i. and Z.C.; writing—original draft preparation, R.N.E.i. and M.O.; writing—review and editing, R.N.E.i., M.O., Z.C. and J.K.; visualization, Z.C. and M.O.; supervision, M.O. and M.M.; project administration, M.O.; funding acquisition J.K. All authors have read and agreed to the published version of the manuscript.

**Funding:** This research received no external funding.

**Conflicts of Interest:** The authors declare no conflict of interest.

## Nomenclature

$i$	EV index
$j$	Home index
$t$	Time index
$T$	Time interval set
$M$	Set of EVs
$N$	Set of buildings
$SoC_{i,min}$	Minimum SoC limit for the EV
$SoC_{i,max}$	Maximum SoC limit for the EV
$SoC_{i,t}^{EV, \text{int}}$	SoC value at arrival time of the $i$ th EV
$SoC_{i,t}^{EV, \text{out}}$	SoC value at departure time of the $i$ th EV
$SoC_i^{exp}$	Expected SoC of the $i$ th EV from the user
$\zeta_{bat,i}^c$	Charging efficiency of the $i$ th EV
$\zeta_{bat,i}^d$	Discharging efficiency of the $i$ th EV

$D_{i,t}^{EV,c}$	Charging decision at time $t$ of the $i$ th EV
$D_{i,t}^{EV,V2L}$	V2L decision at time $t$ of the $i$ th EV
$D_{i,t}^{EV,V2V}$	V2V decision at time $t$ of the $i$ th EV
$t_i^{int}$	Start time of the $i$ th EV
$t_i^{out}$	End time of the $i$ th EV
$l_{basic,t}$	Basic power demand at time $t$
$l_{j,t}^{CD}$	Rated power demand for the CD consumption unit.
$l_{j,t}^{EWH}$	rated power demand for the EWH consumption unit.
$S_{j,t}^{HVAC}$	Decided status for the HVAC unit.
$S_{j,t}^{CD}$	Decided status for the CD unit.
$S_{j,t}^{EWH}$	Decided status for the EWH unit.
$l_{j,t}^{hvac}$	Rated power demand for the HVAC consumption unit.
$l_{j,t}^{EV}$	Rated power demand for the EV consumption unit.
$l_{j,t}^{fixed}$	Fixed power demand for building $j$ .
$\lambda_{i,t}$	Power price at time $t$

## References

- Luo, X.; Zhu, X.; Lim, E.G. Electrical Vehicle-Assisted Demand Side Energy Management. In *Exergy and Its Application—Toward Green Energy Production and Sustainable Environment*; IntechOpen : Tokyo, Japan, 2019.
- Amin, A.; Tareen, W.U.K.; Usman, M.; Ali, H.; Bari, I.; Horan, B.; Mekhilef, S.; Asif, M.; Ahmed, S.; Mahmood, A. A review of optimal charging strategy for electric vehicles under dynamic pricing schemes in the distribution charging network. *Sustainability* **2020**, *12*, 10160.
- Rehman, U.U. Robust Optimization-Based Energy Pricing and Dispatching Model Using DSM for Smart Grid Aggregators to Tackle Price Uncertainty. *Arab. J. Sci. Eng.* **2020**, *45*, 6701–6714. [[CrossRef](#)]
- Kebotogetse, O.; Samikannu, R.; Yahya, A. Review of key management techniques for advanced metering infrastructure. *Int. J. Distrib. Sens. Netw.* **2021**, *17*, 15501477211041541. [[CrossRef](#)]
- Hussain, M.; Gao, Y. A review of demand response in an efficient smart grid environment. *Electr. J.* **2018**, *31*, 55–63. [[CrossRef](#)]
- Zhou, B.; Cao, Y.; Li, C.; Wu, Q.; Liu, N.; Huang, S.; Wang, H. Many-criteria optimality of coordinated demand response with heterogeneous households. *Energy* **2020**, *207*, 118267. [[CrossRef](#)]
- Dogan, A.; Kuzlu, M.; Pipattanasomporn, M.; Rahman, S.; Yalcinoz, T. Impact of EV charging strategies on peak demand reduction and load factor improvement. In Proceedings of the 2015 9th International Conference on Electrical and Electronics Engineering (ELECO), Bursa, Turkey, 26–28 November 2015; pp. 374–378.
- Yadav, M.; Pandey, N.; Jamil, M. Impact of Plug-in Electric Vehicle on Residential Demand Side Management. In Proceedings of the 2020 International Conference on Power Electronics & IoT Applications in Renewable Energy and its Control (PARC), Uttar Pradesh, India, 28–29 February 2020; pp. 365–369.
- Khemakhem, S.; Rekik, M.; Krichen, L. Impact of Electric Vehicles integration on residential demand response system to peak load minimizing in smart grid. In Proceedings of the 2019 19th International Conference on Sciences and Techniques of Automatic Control and Computer Engineering (STA), Sousse, Tunisia, 24–26 March 2019; pp. 572–577.
- Ferreira, J.C.; Monteiro, V.; Afonso, J.L. Vehicle-to-everything application (V2Anything App) for electric vehicles. *IEEE Trans. Ind. Inform.* **2013**, *10*, 1927–1937. [[CrossRef](#)]
- Thompson, A.W.; Perez, Y. Vehicle-to-Everything (V2X) energy services, value streams, and regulatory policy implications. *Energy Policy* **2020**, *137*, 111136. [[CrossRef](#)]
- Xi, X.; Sioshansi, R. Using price-based signals to control plug-in electric vehicle fleet charging. *IEEE Trans. Smart Grid* **2014**, *5*, 1451–1464. [[CrossRef](#)]
- Mahat, P.; Handl, M.; Kanstrup, K.R.; Lozano, A.P.; Sleimovits, A. Price based electric vehicle charging. In Proceedings of the 2012 IEEE Power and Energy Society General Meeting, San Diego, CA, USA, 22–26 July 2012; pp. 1–8.
- Limmer, S.; Rodemann, T. Peak load reduction through dynamic pricing for electric vehicle charging. *Int. J. Electr. Power Energy Syst.* **2019**, *113*, 117–128. [[CrossRef](#)]
- Mehta, R.; Srinivasan, D.; Trivedi, A.; Yang, J. Hybrid planning method based on cost-benefit analysis for smart charging of plug-in electric vehicles in distribution systems. *IEEE Trans. Smart Grid* **2017**, *10*, 523–534. [[CrossRef](#)]
- Tan, J.; Wang, L. Integration of plug-in hybrid electric vehicles into residential distribution grid based on two-layer intelligent optimization. *IEEE Trans. Smart Grid* **2014**, *5*, 1774–1784. [[CrossRef](#)]
- Nguyen, V.L.; Tran-Quoc, T.; Bacha, S.; Nguyen, B. Charging strategies to minimize the peak load for an electric vehicle fleet. In Proceedings of the IECON 2014-40th Annual Conference of the IEEE Industrial Electronics Society, Dallas, TX, USA, 29 October–1 November 2014; pp. 3522–3528.
- Yang, Y.; Wang, S. Resilient residential energy management with vehicle-to-home and photovoltaic uncertainty. *Int. J. Electr. Power Energy Syst.* **2021**, *132*, 107206. [[CrossRef](#)]

19. Mbungu, N.T.; Ismail, A.A.; Bansal, R.C.; Hamid, A.K.; Naidoo, R.M. An optimal energy management scheme of a vehicle to home. In Proceedings of the 2022 IEEE 21st Mediterranean Electrotechnical Conference (MELECON), Palermo, Italy, 14–16 June 2022; pp. 1056–1060.
20. Heinisch, V.; Göransson, L.; Erlandsson, R.; Hodel, H.; Johnsson, F.; Odenberger, M. Smart electric vehicle charging strategies for sectoral coupling in a city energy system. *Appl. Energy* **2021**, *288*, 116640. [[CrossRef](#)]
21. Ismail, A.A.; Mbungu, N.T.; Elnady, A.; Bansal, R.C.; Hamid, A.K.; AlShabi, M. Impact of electric vehicles on smart grid and future predictions: A survey. *Int. J. Model. Simul.* **2022**, 1–17. [[CrossRef](#)]
22. Li, G.; Boukhatem, L.; Zhao, L.; Wu, J. Direct vehicle-to-vehicle charging strategy in vehicular ad-hoc networks. In Proceedings of the 2018 9th IFIP International Conference on New Technologies, Mobility and Security (NTMS), Paris, France, 26–28 February 2018; pp. 1–5.
23. El Idrissi, R.N.; Ouassaid, M.; Maaroufi, M. A Constrained Programming-Based Algorithm for Optimal Scheduling of Aggregated EVs Power Demand in Smart Buildings. *IEEE Access* **2022**, *10*, 28434–28444. [[CrossRef](#)]
24. Tang, Y.; Chen, Q.; Ning, J.; Wang, Q.; Feng, S.; Li, Y. Hierarchical control strategy for residential demand response considering time-varying aggregated capacity. *Int. J. Electr. Power Energy Syst.* **2018**, *97*, 165–173. [[CrossRef](#)]
25. El Idrissi, R.N.; Ouassaid, M.; Maaroufi, M. Collective demand side management in smart grids. In Proceedings of the 2020 5th International Conference on Renewable Energies for Developing Countries (REDEC), Marrakech, Morocco, 29–30 June 2020; pp. 1–6.
26. El Idrissi, R.N.; Ouassaid, M.; Maaroufi, M. An intelligent demand side management algorithm for smart buildings. In Proceedings of the 2021 12th International Renewable Engineering Conference (IREC), Amman, Jordan, 14–15 April 2021; pp. 1–6.
27. Gurobi Optimizer. Gurobi Optimizer Description. Available online: <https://www.gurobi.com/faqs/mip-for-data-scientists/> (accessed on 1 December 2022).
28. Mao, T.; Zhang, X.; Zhou, B. Modeling and solving method for supporting ‘vehicle-to-anything’ EV charging mode. *Appl. Sci.* **2018**, *8*, 1048. [[CrossRef](#)]
29. Chen, J.; Zhang, Y.; Li, X.; Sun, B.; Liao, Q.; Tao, Y.; Wang, Z. Strategic integration of vehicle-to-home system with home distributed photovoltaic power generation in Shanghai. *Appl. Energy* **2020**, *263*, 114603. [[CrossRef](#)]

**Disclaimer/Publisher’s Note:** The statements, opinions and data contained in all publications are solely those of the individual author(s) and contributor(s) and not of MDPI and/or the editor(s). MDPI and/or the editor(s) disclaim responsibility for any injury to people or property resulting from any ideas, methods, instructions or products referred to in the content.